Chinese Chemical Letters 34 (2023) 107344

Contents lists available at ScienceDirect

Chinese Chemical Letters

journal homepage: www.elsevier.com/locate/cclet

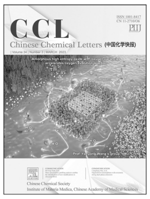

Oxidation-responsive framboidal triblock copolymer vesicles prepared by photoinitiated RAFT seeded emulsion polymerization

Jun He[a], Ying Chen[b], Li Zhang[a,b], Jianbo Tan[a,b,*]

[a] *Department of Polymeric Materials and Engineering, School of Materials and Energy, Guangdong University of Technology, Guangzhou 510006, China*
[b] *Guangdong Provincial Key Laboratory of Functional Soft Condensed Matter, Guangzhou 510006, China*

ARTICLE INFO

Article history:
Received 2 February 2022
Revised 8 March 2022
Accepted 15 March 2022
Available online 21 March 2022

Keywords:
RAFT polymerization
Block copolymer
Vesicles
Oxidation-responsive
Emulsion polymerization

ABSTRACT

Stimulus-responsive vesicles have broad applications in a variety of areas. Herein, oxidation-responsive framboidal triblock copolymer vesicles are prepared by photoinitiated RAFT seeded emulsion polymerization of a thioether-functionalized monomer using diblock copolymer vesicles as seeds. The obtained framboidal vesicles can transform into worms or spheres in the presence of reactive oxygen species, which can be further used for controlled release of cargos (*e.g.*, silica nanoparticles).

Polymer vesicles comprise a polymeric bilayer membrane have attracted increasing attentions due to their potential applications in biomineralization, drug delivery, theranostics, catalysis, nanoreactors and so on [1–5]. It is well-known that amphiphilic block copolymers can self-assemble in water to form vesicles with suitable volume fractions of each block [6]. However, this post-polymerization processing method is usually conducted in a highly dilute solution (<1% w/w solids), which is difficult to implement on an industrial scale.

Recently, polymerization-induced self-assembly (PISA) combined with reversible addition-fragmentation chain transfer (RAFT) polymerization has provided a versatile platform to prepare concentrated polymer vesicles (10%−45%, w/w) in different solvents such as water, alcohol, non-polar solvents [7–16]. Moreover, the rich RAFT reactive groups embedded inside the vesicular membrane enable one to further tune the composition and morphology of vesicles *via* further chain extension [17–19]. For example, Armes group [19] reported the first preparation of triblock copolymer vesicles with a framboidal morphology by introducing nanoscale phase separation into vesicular membrane of poly(glycerol monomethacrylate)-*b*-poly(2-hydroxypropyl methacrylate) (PGMA-PHPMA) vesicles *via* RAFT seeded emulsion polymerization. These framboidal vesicles could be used as efficient emulsifiers for Pickering emulsions [20], substrates for the preparation of inorganic/organic nanocomposites [21] or carriers for gene delivery [22]. Despite some progresses have been made in framboidal vesicles, the preparation of stimulus-responsive framboidal vesicles by RAFT-mediated PISA has rarely been reported. To the best of our knowledge, only recently pH-responsive triblock copolymer framboidal vesicles have been prepared by using poly(2-(diisopropylamino)ethyl methacrylate) (PDPA) as the third block [23]. Given the unique morphology and potential applications of framboidal vesicles, it is highly desirable to expand the scope of stimulus-responsive framboidal vesicles prepared by PISA.

In this communication, we reported the first preparation of oxidation-responsive framboidal triblock copolymer vesicles by photoinitiated RAFT seeded emulsion polymerization of 2-(methylthio)ethyl methacrylate (MTEMA) at room temperature using PHPMA-based vesicles as seeds. As shown in Scheme 1, 4-cyano-4-(ethylthiocarbonothioylthio)pentanoic acid (CEPA) modified monomethoxy poly(ethylene glycol) (mPEG$_{113}$, $M_n = 5000$ g/mol) was employed to mediate photoinitiated RAFT dispersion polymerization of HPMA (20% w/w, target degree of polymerization (DP) of 400) in water at room temperature. The polymerization was performed under purple light irradiation ($\lambda = 405$ nm, 0.50 mW/cm^2) using sodium phenyl 2,4,6-trimethylbenzoylphosphinate (SPTP) as the photoinitaitor. Similar to our previous research [24], pure vesicles were obtained for the mPEG$_{113}$-PHPMA$_{400}$ formulation. The obtained mPEG$_{113}$-PHPMA$_{400}$ vesicles were further used as seeds for photoinitiated RAFT seeded polymerization of MTEMA at room temperature to prepare fram-

---

[*] Corresponding author at: Department of Polymeric Materials and Engineering, School of Materials and Energy, Guangdong University of Technology, Guangzhou 510006, China.

E-mail address: tanjianbo@gdut.edu.cn (J. Tan).

https://doi.org/10.1016/j.cclet.2022.03.067

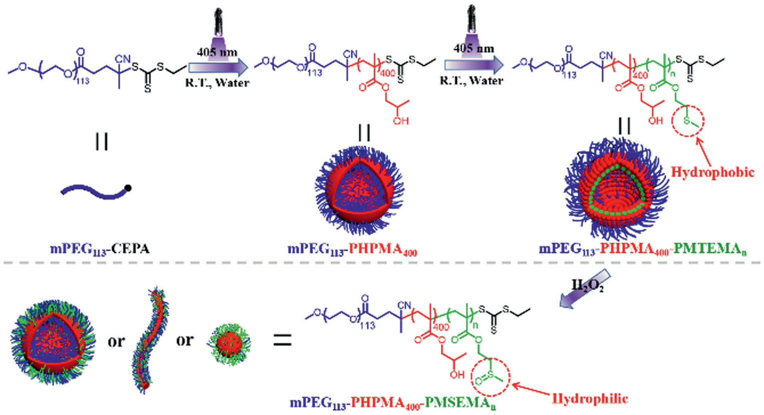

Scheme 1. Schematic illustration for the preparation of mPEG$_{113}$-PHPMA$_{400}$ vesicles by aqueous photoinitiated RAFT dispersion polymerization of HPMA using mPEG$_{113}$–CEPA and framboidal mPEG$_{113}$-PHPMA$_{400}$-PMTEMA$_{n}$ vesicles by photoinitiated RAFT seeded emulsion polymerization of MTEMA using mPEG$_{113}$-PHPMA$_{400}$ vesicles as seeds.

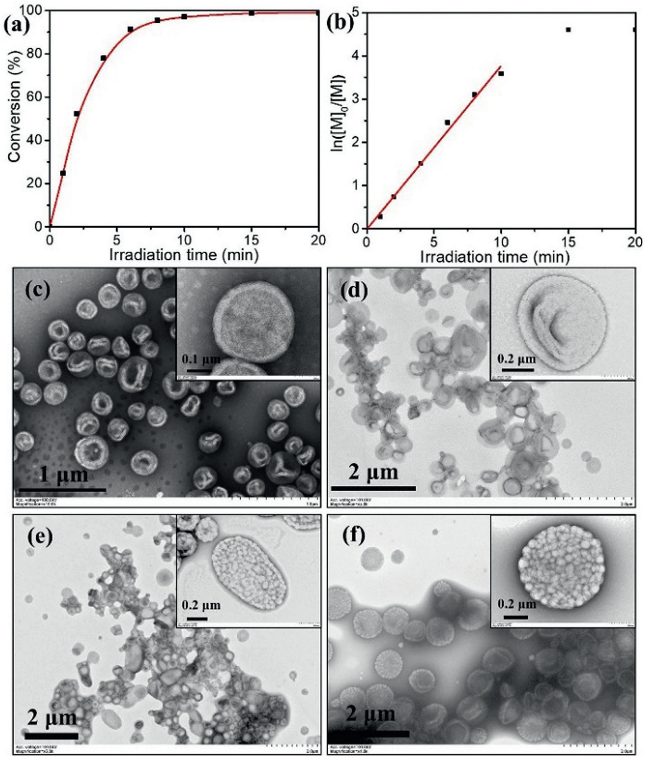

Fig. 1. (a) Polymerization kinetics of photoinitiated RAFT seeded emulsion polymerization of MTEMA (target DP of 300) using mPEG$_{113}$-PHPMA$_{400}$ vesicles as seeds. (b) Plots of $\ln([M]_0/[M])$ *vs.* irradiation time derived from the data of Fig. 1a. (c) TEM image of mPEG$_{113}$-PHPMA$_{400}$ vesicles prepared by aqueous photoinitiated RAFT dispersion polymerization. TEM images of mPEG$_{113}$-PHPMA$_{400}$-PMTEMA$_{n}$ vesicles prepared by photoinitiated RAFT seeded emulsion polymerization of MTEMA: (d) $n = 100$, (e) $n = 200$, (f) $n = 300$.

boidal triblock copolymer vesicles. Since MTEMA is a hydrophobic monomer, the polymerization should proceed under seeded emulsion polymerization conditions.

Fig. 1a shows polymerization kinetics of the photoinitiated RAFT seeded emulsion polymerization of MTEMA (target DP of 300). The polymerization exhibited an ultrafast polymerization behavior, with 91.4% and 99.0% monomer conversion being achieved within 6 and 15 min of light irradiation, respectively. This can be attributed to the relatively short half-life of SPTP under purple light irradiation [25]. Moreover, corresponded $\ln([M]_0/[M])$ increased linearly with irradiation time $\leq$10 min (Fig. 1b), suggesting a controlled/"living" polymerization mechanism. When the irradiation time was $>$10 min, the monomer conversion was high ($>$97%) and $\ln([M]_0/[M])$ did not fit the linear relationship. Samples of mPEG$_{113}$-PHPMA$_{400}$-PMTEMA$_{n}$ ($n = 0$, 100, 200, 300) were characterized by transmission electron microscopy (TEM) (Figs. 1c–f). It was found that vesicular morphology was maintained in each case. Moreover, after the chain extension of PMTEMA, the surface of vesicles becomes increasingly rough and individual globules of ~40 nm was observed when the DP of PMTEMA reached 200. This result reveals that nanoscale phase separation occurs within the vesicular membrane during the polymerization of MTEMA due to the incompatibility between the weakly hydrophobic PHPMA block and the strongly hydrophobic PMTEMA. As the DP of PMTEMA was increased from 200 to 300, the globules in the vesicles grew both in prominence and size.

As reported by Armes group and our group [20,21], framboidal vesicles prepared by RAFT seeded emulsion polymerization can be used as efficient emulsifiers for Pickering emulsion. The framboidal mPEG$_{113}$-PHPMA$_{400}$-PMTEMA$_{n}$ ($n = 100$, 200, 300) triblock copolymer vesicles and the mPEG$_{113}$-PHPMA$_{400}$ diblock copolymer vesicles were further evaluated as Pickering emulsifiers for the stabilization of hexane-in-water emulsions. Aqueous dispersions of these vesicles (0.1% to 2.0%, w/w) were homogenized with an equal volume of hexane at 12,000 rpm for 2 min to form stable Pickering emulsions (Figs. S4–S7 in Supporting information). Mean diameters of the resulting emulsions were determined by optical microscopy. Fig. 2 shows optical microscopy images of emulsions as stabilized with different concentrations of mPEG$_{113}$-PHPMA$_{400}$ diblock copolymer vesicles (Figs. 2a–d) and framboidal mPEG$_{113}$-PHPMA$_{400}$-PMTEMA$_{300}$ triblock copolymer vesicles (Figs. 2e–h). It was found that emulsions stabilized with mPEG$_{113}$-PHPMA$_{400}$ diblock copolymer vesicles were clearly larger than those stabilized with framboidal mPEG$_{113}$-PHPMA$_{400}$-PMTEMA$_{300}$ triblock copolymer vesicles. Fig. 2i shows the concentration dependence of mean diameters of the resulting emulsions, which is typically observed in Pickering emulsion. Moreover, it was found that increasing the DP of PMTEMA led to lower limiting concentrations of vesicles as well as emulsions with smaller sizes. These results suggest that mPEG$_{113}$-PHPMA$_{400}$-PMTEMA$_{n}$ ($n = 0$, 100, 200, 300) vesicles with higher DP of PMTEMA are more efficient emulsifier, since less vesicles were required to stabilize hexane droplets. This can be attributed to the increased surface roughness and hydrophobicity of framboidal mPEG$_{113}$-PHPMA$_{400}$-PMTEMA$_{n}$ triblock copolymer vesicles with increasing PMTEMA fraction [20].

It is well-known that thioether moiety can transform into corresponding sulfoxide or sulfone moiety *via* the oxidation by reactive oxygen species (ROS) (*e.g.*, hydrogen peroxide (H_2O_2)) [26].

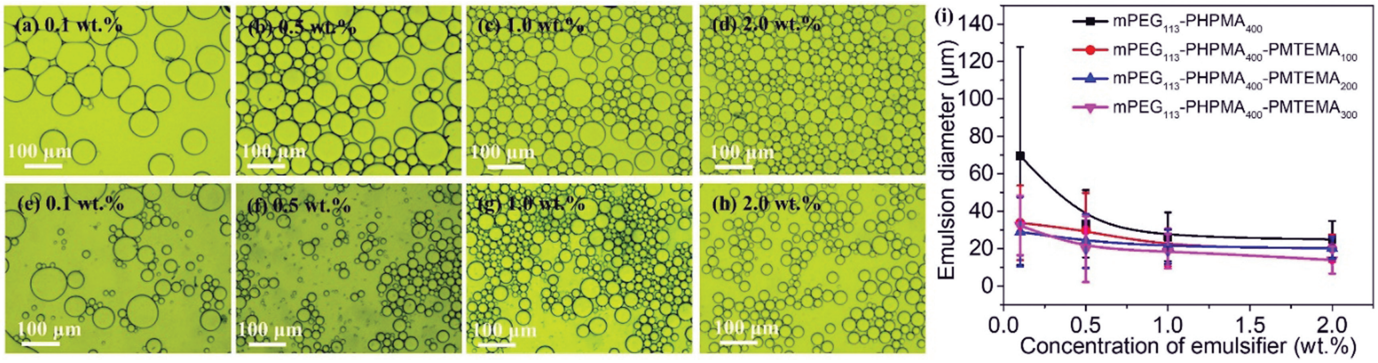

Fig. 2. Optical microscopy images of emulsions stabilized with different concentrations of (a-d) mPEG_{113}-PHPMA_{400} vesicles and (e-h) framboidal mPEG_{113}-PHPMA_{400}-PMTEMA_{300} vesicles. (i) Evolution of diameter of emulsions with the concentration of mPEG_{113}-PHPMA_{400}-PMTEMA_{n} ($n = 0$, 100, 200, 300) vesicles for hexane-in-water Pickering emulsion.

Therefore, thioether-functionalized polymers can be used to regulate ROS in some diseases such as cancer, diabetes [27]. Moreover, hydrophobic thioether-functionalized polymers can be used to construct oxidation-responsive vesicles due to the change of the hydrophobic thioether moiety to the hydrophilic sulfoxide *via* oxidation [28,29]. We hypothesized that the obtained framboidal mPEG_{113}-PHPMA_{400}-PMTEMA_{n} vesicles could exhibit oxidation-responsive behavior due to the increased hydrophilicity of the formed sulfoxide-functionalized block (poly(methylsulfinyl)ethyl methacrylate, PMSEMA). To test this hypothesis, a certain volume of aqueous solution of H_2O_2 (30 wt%) was added into an aqueous solution of framboidal mPEG_{113}-PHPMA_{400}-PMTEMA_{300} vesicles and the kinetics of oxidation was followed by ^{1}H NMR spectroscopy. As shown in Figs. S8 and S9 (Supporting information), thioether moieties of the PMTEMA block can completely transform into sulfoxide moieties after treating with H_2O_2 for 9 h. To further evaluate the change of morphologies of framboidal mPEG_{113}-PHPMA_{400}-PMTEMA_{n} vesicles after oxidation, these vesicles were treated with H_2O_2 for 24 h and characterized by TEM and dynamic light scattering (DLS). When the DP of PMTEMA was 100, the vesicular morphology was retained after treating with H_2O_2 (Fig. 3a). DLS results showed that the hydrodynamic diameter of vesicles was almost the same before and after H_2O_2 treatment (Fig. 3b). This is because the enhanced hydrophilic character gained by the PMSEMA as a result of oxidation of PMTEMA is not sufficient to induce a morphological transition. In contrast, targeting higher PMTEMA DPs of either 200 or 300 enables access for the morphological transition from framboidal vesicles to either branched worms (Fig. 3c) or spheres mixed with branched worms (Fig. 3e). In the case of the framboidal mPEG_{113}-PHPMA_{400}-PMTEMA_{200} vesicles, a significant increase in the intensity-average diameter from 323.6 nm to 466.6 nm is observed after the H_2O_2 treatment (Fig. 3d), which provides good evidence for a vesicle-to-branched worm transition. A different trend was observed for the case of framboidal mPEG_{113}-PHPMA_{400}-PMTEMA_{300} vesicles, which undergoes a vesicle-to-sphere transition with a reduction in hydrodynamic diameter from 519.3 to 187.5 nm after H_2O_2 treatment (Fig. 3f).

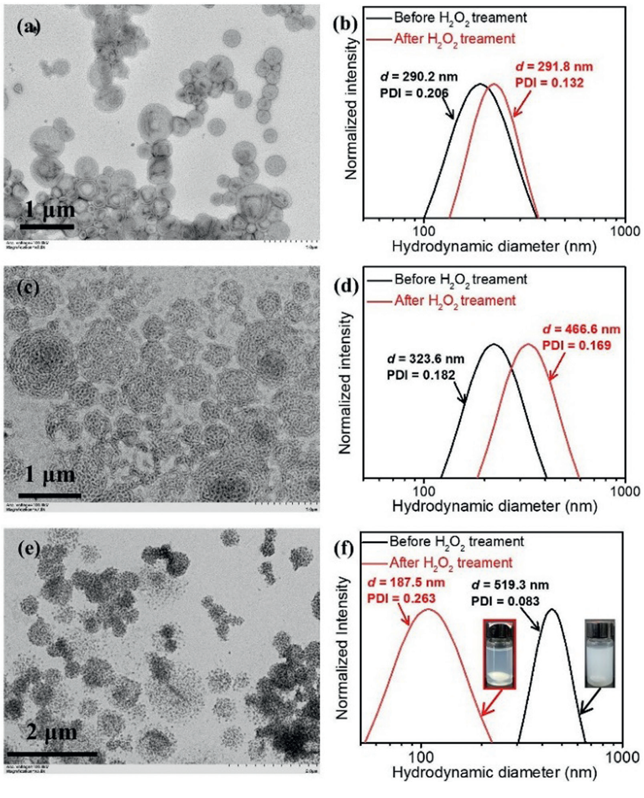

Fig. 3. (a, c, e) TEM images of mPEG_{113}-PHPMA_{400}-PMTEMA_{n} ($n = 100$, 200, 300) vesicles after treating with H_2O_2 for 24 h and (b, d, f) DLS particle size distributions of mPEG_{113}-PHPMA_{400}-PMTEMA_{n} ($n = 100$, 200, 300) vesicles before and after treating with H_2O_2 for 24 h: (a, b) $n = 100$, (c, d) $n = 200$, (e, f) $n = 300$.

Polymer vesicles that can release cargos from the lumen have potential to be smart carriers or nanoreactors for various applications [30,31]. The framboidal mPEG_{113}-PHPMA_{400}-PMTEMA_{n} ($n = 200$, 300) vesicles prepared by photoinitiated RAFT seeded emulsion polymerization can undergo vesicle-to-worm or vesicle-to-sphere transition via oxidation, which can be employed to trigger the on-demand release of cargos loaded inside vesicles. Herein, silica nanoparticles with a diameter of 20 nm were used as model cargos to investigate the oxidation-responsive release behavior of the framboidal vesicles (Fig. 4a). According to our previous research [32], silica nanoparticles-loaded vesicles could be prepared by aqueous photoinitiated RAFT dispersion polymerization of HPMA (20% w/w, target DP of 400) with silica nanoparticles added at the beginning of the polymerization (Fig. 4b). After the complete conversion of HPMA, additional amounts of MTEMA, SPTP, and water were added into the reaction mixture for further chain extension under RAFT seeded emulsion polymerization conditions (targe DP of PMTEMA of 300). The obtained samples were purified by several centrifugation-redispersion cycles to remove unloaded silica nanoparticles. TEM and thermogravimetric analyzer (TGA) characterizations confirmed the formation of silica nanoparticles-loaded framboidal triblock copolymer vesicles (Fig. 4c and Fig. S10 in Supporting information). For silica nanoparticles-loaded framboidal triblock copolymer vesicles, the loaded silica nanoparticles

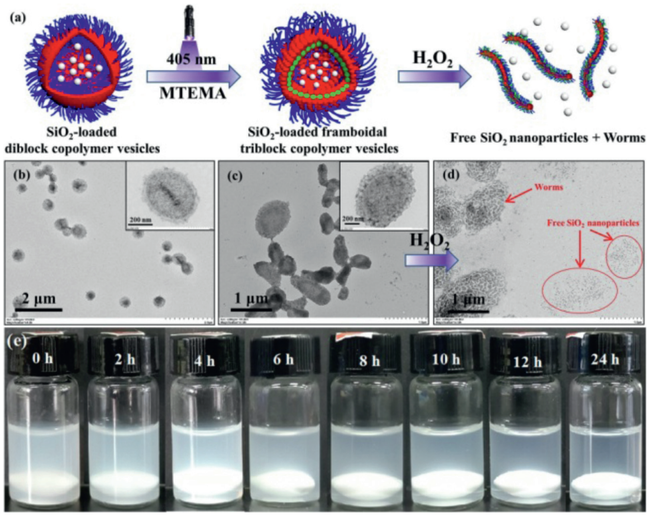

Fig. 4. (a) Schematic illustration for the preparation of silica nanoparticles-loaded framboidal vesicles and the subsequent release of silica nanoparticles with the addition of H_2O_2. (b) TEM image of silica nanoparticles-loaded mPEG$_{113}$-PHPMA$_{400}$ vesicles. (c) TEM image of silica nanoparticles-loaded framboidal mPEG$_{113}$-PHPMA$_{400}$-PMTEMA$_{300}$ vesicles. (d) TEM image of the sample after treating silica nanoparticles-loaded framboidal mPEG$_{113}$-PHPMA$_{400}$-PMTEMA$_{300}$ vesicles with H_2O_2 for 24 h. (e) Digital images of aqueous dispersions of silica nanoparticles-loaded framboidal mPEG$_{113}$-PHPMA$_{400}$-PMTEMA$_{300}$ vesicles after the addition of H_2O_2 at different times.

were fully released after 24 h in the presence of H_2O_2 due to the transformation of vesicles into worms (Fig. 4d). The original dispersion of silica nanoparticles-loaded framboidal vesicles became less turbid after the addition of H_2O_2 as a result of the vesicle-to-worm transition (Fig. 4e).

In summary, we demonstrate the preparation of oxidation-responsive framboidal triblock copolymer vesicles by photoinitiated RAFT seeded emulsion polymerization of MTEMA using mPEG$_{113}$-PHPMA$_{400}$ vesicles as seeds. The obtained framboidal vesicles could serve as efficient emulsifiers for Pickering emulsion. Moreover, these framboidal vesicles exhibited oxidation-responsive properties and could transform into worms or spheres in the presence of H_2O_2 for controlled release of silica nanoparticles.

Declaration of competing interest

The authors declare that they have no known competing financial interests or personal relationships that could have appeared to influence the work reported in this paper

Acknowledgments

The authors acknowledge support from the Science and Technology Program of Guangzhou (No. 202102020631), the National Natural Science Foundation of China (Nos. 22171055 and 21971047) and Innovation Project of Education Department in Guangdong (No. 2018KTSCX053). Y. Chen acknowledges the support from Guangdong Special Support Program (No. 2017TX04N371).

Supplementary materials

Supplementary material associated with this article can be found, in the online version, at doi:10.1016/j.cclet.2022.03.067.

References

[1] Y. Zhu, B. Yang, S. Chen, J. Du, Progr. Polym. Sci. 64 (2017) 1–22.
[2] L.D. Blackman, S. Varlas, M.C. Arno, et al., ACS Cent. Sci. 4 (2018) 718–723.
[3] S.F.M. van Dongen, W.P.R. Verdurmen, R.J.R.W. Peters, et al., Angew. Chem. Int. Ed. 49 (2010) 7213–7216.
[4] Z. Wang, M.C.M. van Oers, F.P.J.T. Rutjes, J.C.M. van Hest, Angew. Chem. Int. Ed. 51 (2012) 10746–10750.
[5] Y. Deng, H. Chen, X. Tao, et al., Chin. Chem. Lett. 31 (2020) 1931–1935.
[6] Y. Mai, A. Eisenberg, Chem. Soc. Rev. 41 (2012) 5969–5985.
[7] S.L. Canning, G.N. Smith, S.P. Armes, Macromolecules 49 (2016) 1985–2001.
[8] N.J.W. Penfold, J. Yeow, C. Boyer, S.P. Armes, ACS Macro Lett. 8 (2019) 1029–1054.
[9] X. Wang, L. Shen, Z. An, Progr. Polym. Sci. 83 (2018) 1–27.
[10] F. D'Agosto, J. Rieger, M. Lansalot, Angew. Chem. Int. Ed. 59 (2020) 8368–8392.
[11] D. Liu, J. He, L. Zhang, J. Tan, ACS Macro Lett. 8 (2019) 1660–1669.
[12] J. Cao, Y. Tan, Y. Chen, L. Zhang, J. Tan, Macromol. Rapid Commun. 42 (2021) 2100498.
[13] C.A. Figg, A. Simula, K.A. Gebre, et al., Chem. Sci. 6 (2015) 1230–1236.
[14] Y. Cao, Y. Shi, X. Wu, L. Zhang, Chin. Chem. Lett. 31 (2020) 1660–1664.
[15] X. Zhang, J. Gao, X. Zhao, et al., Chin. Chem. Lett. 31 (2020) 1822–1826.
[16] W.B. Cai, D.D. Liu, Y. Chen, L. Zhang, J.B. Tan, Chin. J. Polym. Sci. 39 (2021) 1127–1137.
[17] H. Zhou, C. Liu, Y. Qu, et al., Macromolecules 49 (2016) 8167–8176.
[18] J. He, J. Cao, Y. Chen, L. Zhang, J. Tan, ACS Macro Lett. 9 (2020) 533–539.
[19] P. Chambon, A. Blanazs, G. Battaglia, S.P. Armes, Macromolecules 45 (2012) 5081–5090.
[20] C.J. Mable, N.J. Warren, K.L. Thompson, O.O. Mykhaylyk, S.P. Armes, Chem. Sci. 6 (2015) 6179–6188.
[21] Q. Xu, Y. Zhang, X. Li, et al., Polym. Chem. 9 (2018) 4908–4916.
[22] C.J. Mable, I. Canton, O.O. Mykhaylyk, et al., Chem. Sci. 10 (2019) 4811–4821.
[23] C.J. Mable, L.A. Fielding, M.J. Derry, et al., Chem. Sci. 9 (2018) 1454–1463.
[24] D. Liu, Y. Chen, L. Zhang, J. Tan, Macromolecules 53 (2020) 9725–9735.
[25] Y. Du, S. Jia, Y. Chen, L. Zhang, J. Tan, ACS Macro Lett. 10 (2021) 297–306.
[26] A.A. Ghogare, A. Greer, Chem. Rev. 116 (2016) 9994–10034.
[27] D. Zhang, Y. Wei, K. Chen, et al., Adv. Healthc. Mater. 4 (2015) 69–76.
[28] S. Xu, G. Ng, J. Xu, et al., ACS Macro Lett. 6 (2017) 1237–1244.
[29] F.H. Sobotta, M.T. Kuchenbrod, F.V. Gruschwitz, et al., Angew. Chem. Int. Ed. 60 (2021) 24716–24723.
[30] A. Feng, J. Yuan, Macromol. Rapid Commun. 35 (2014) 767–779.
[31] H. Che, J.C.M. van Hest, J. Mater. Chem. B 4 (2016) 4632–4647.
[32] J. Tan, H. Sun, M. Yu, B.S. Sumerlin, L. Zhang, ACS Macro Lett. 4 (2015) 1249–1253.